G.V. Lashkarev[1], P.V. Demydiuk[1], G.Yu. Yurkov[2], O.I. Dmitriev[1], O.I. Bykov[1], L.I. Klochkov[1], Y.P. Pyratinskiy[3], E.I. Slynko[1], A.G. Khandozhko[4], O.V. Popkov[2], N.A. Taratanov[2]

[1]Frantsevich Institute for Problems of Material Science, National Academy of Science of Ukraine
Krzhyzhanovsky str., 3, Kiev, 03142, Ukraine

[2]A.A. Baikov Institute of Metallurgy and Materials Science of Russian academy of science
Leninsky prospect, 49, Moscow, 119991, Russia

[3]Institute of Physics, National Academy of Science of Ukraine
Prospect Nauky, 46, Kiev, 03650, Ukraine

[4]Yuriy Fedkovich Chernivtsi National University
Kotsiubynskogo str., 2, Chernivtsi, 58012, Ukraine

PROPERTIES OF NANOPARTICLES ZnO:Mn IMMOBILIZED IN POLYETHYLENE MATRIX

Key words: *nanoparticle, ZnO, Mn, photoluminescence, luminescence, ESR*

Nanoparticles ZnO:Mn (3–5nm) immobilized in polyethylene matrix were synthesized. The samples with different content of the manganese (5, 10 and 20%) in the initial solution of the Mn and Zn precursors were investigated by means of ESR, PL and XRD. Thus the behavior of the Mn impurities in ZnO was studied. It was observed that most of the manganese in ZnO form second undefined phase MnO_x or substitute the zinc in cation sublattice at the surface layer of the nanoparticles. The mean value of constant of hyperfine structure of Mn is higher than expected one (<A> = $(94\pm3)\cdot10^{-4}$ cm^{-1}) that is significantly differ from the constant of hyperfine structure of Mn incorporated into single crystal ZnO ($76\cdot10^{-4}$ cm^{-1}). Photoluminescence measurements has revealed wide band of emission in green-red region 500–600 nm, with different position of the maximum depending on the manganese content.

Introduction

Onrush of nanotechnology gives rise to reconsideration of functional capacity of well-known materials. In particular many papers have been dedicated to the research on nanosized systems that are based on zinc oxide.

ZnO is a direct wide-gap (3.37 eV) semiconductor with extremely high exciton binding energy (60 meV). In addition it is nonexpensive, nontoxic and

resistive to the high energy radiation [1]. These features should create prerequisites for ZnO to be applied in crystalophosphors as work medium for luminescent centers. Quantitative characteristics of such optical system are altered with transition to nanoscale as a result of profound influence of confinement effects and surface states. The former is based on effect of surface restriction that in turn acts as potential barrier with endless walls.

As a result, confinement effect leads to increasing of band gap, binding energy of exciton and overlapping of electron-hole wave functions. Each mentioned effect makes its positive contribution to quantum efficiency of the crystalophosphors what consists in increasing of oscillator strength of band-to-band transition, lifetime of exciton and probability of their interaction with luminescent centers [2].

In order to research such system, nanoparticles (NP) ZnO:Mn^{2+} immobilized in polyethylene matrix (hereafter *Samples*) were synthesized. Manganese is expected to be center of yellow-green luminescence (~580 nm) due to $^4T_1(G) - {}^6A_1$ transition in crystal field of hexagonal symmetry [3] (for example ZnS). Moreover orbital and spin quantum numbers of Mn^{2+} in ground state are $L = 0$ and $S = 5/2$. Therefore it is also proper element for probing of local surroundings in the host by means of ESR (Mn^{2+} has six lines of hyperfine structure). That is very important upon studying of doped nanoparticles.

As for the synthesis process the mixture of precursors containing Zn^{2+} and Mn^{2+} ions was introduced into the solution of polyethylene in hydrocarbon oil. Thus separated particles were protected from agglomeration and atmospheric impact. It was also observed that behavior of the NP had been correlated by option of zinc and manganese precursors. Therefore influence of mixtures of precursors Zn(NO$_3$)$_2$ with Mn(NO$_3$)$_2$ and Zn(CH$_3$COO)$_2$ with Mn(CH$_3$COO)$_2$ on the NP properties was studied.

Experement

Synthesis

Investigated NPs were synthesized in compliance with the methodology that was described elsewhere [4, 5]. A water solution of Zn and Mn precursors with the concentration varying from 0.05 to 0.06 mol/l

was prepared. LDPE (low density polyethylene) was dissolved in mineral oil in argon atmosphere using intensive stirring and heating. A solution of precursors was being introduced dropwise into the reaction mass for 24 h at 250 °C. Throughout a synthesis, gaseous products of the reaction and residual water were removed from the reaction vessel by an argon stream. Afterwards, a reaction mass (polymer-nanoparticles-oil) was stirred at a proper temperature for 40 min with the purpose to complete thermal decomposition of the initial precursors, then cooled down to room temperature and placed into a Soxhlet extractor where residual oil was completely removed.

Two groups of *Samples* were prepared. Zn(NO$_3$)$_2$ with Mn(NO$_3$)$_2$ and Zn(CH$_3$COO)$_2$ with Mn(CH$_3$COO)$_2$ were used as the zinc and manganese precursors for preparation of the first and second groups of samples, respectively. Three types of *Samples* that were synthesized from initial solution of precursors containing 5, 10, and 20 %wt. of Mn were studied in both groups (Table 1).

However the initial solution of the precursors consists of particular amount of the manganese, its actual concentration in final nanoparticles ZnO is under question and may strongly diverge from the initial value. Within this paper it is considered that value of the manganese concentration in nanoparticles ZnO is less than 1%. This assumption is made on the base of ESR measurements, that have shown six line of the hyperfine structure (Fig. 5), that means low amount (<1%) of magnetic ions have been introduced into the nanoparticles ZnO. As for the localization of the rest part of manganese it seems to form some oxygen phase MnO$_x$. Its presence is indicated by X-ray diffraction measurement (Fig. 2 the band under notation MnO$_x$).

Measurement equipment

X-ray diffraction measurements (XRD) were performed with modified computer-controlled diffractometer DRON-3M equipped with X-ray tube BSV-28, cupper anode ($\lambda = 1.54$ μkm) and nickel filter. Data processing was performed according to the database of standard XRD spectrum value ASTM (American Society of Testing Materials).

Table 1. **List of synthesized *Samples***

Precursor	I group			II group		
	$Zn(NO_3)_2 + Mn(NO_3)_2$			$Zn(CH_3COO)_2 + Mn(CH_3COO)_2$		
Samples	N1	N2	N3	N4	N5	N6
Content of manganeses, %	5	10	20	5	10	20

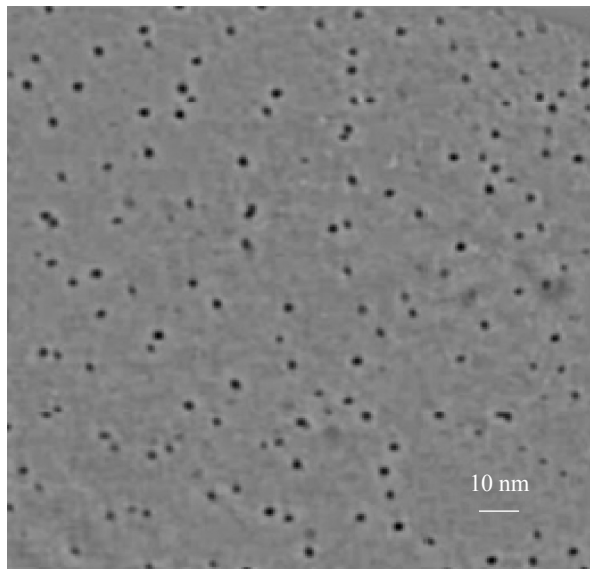The ESR experiments were performed at *X* band ~10 GHz at room temperature.

Fig. 1. TEM image of ZnO:Mn nanoparticles. The average size of the NP is 3–5 nm
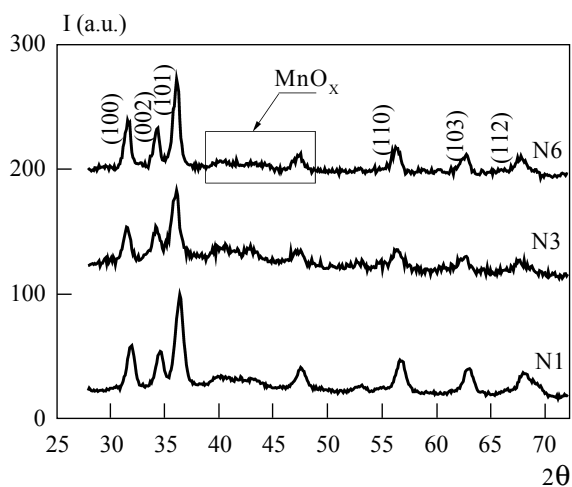

Fig. 2. XRD spectrum for Samples N1, N3, N6

Photoluminescence (PL) spectra were excited by nitrogen laser (337 nm) and measured at room temperature.

Results and discussion

Six *Samples* were synthesized (Table 1). The average size of NP was estimated using TEM instrument (Fig. 1) and assigned to be 3–5 nm. Basing on minimum energy principle for surface strain and TEM image (Fig.1) the NPs are suggested to have sphere like shape.

The XRD pattern exhibited a wurtzite structure of ZnO (Fig. 2), for both groups of *Samples*. Two *Samples* with the highest content of manganese (20%) from every of the groups (N3 and N6) and one *Sample* N1 (5% Mn) were chosen to compare with one another. As it can be seen from Fig. 2 they have particularly identical XRD spectra that are characterized by six lines of ZnO hexagonal structure and weak unidentified lines with $2\theta = 38 \div 49°$. According to the ASTM these unknown lines can be assigned to be compounds of manganese with oxygen. Thus we could hardly give unambiguous answer what these phases are, so hereinafter they are referred as MnO_x (Manganese oxide).

A comparative analysis of XRD spectra for N1, N3 and N6 was performed. To reveal difference between these *Samples*, two parameters for each spectrum were estimated. First parameter is a interplanar spacing of crystalline structures, calculated by Bragg's equation (Fig. 3):

$$d = \frac{\lambda}{2 \cdot \sin\theta} \qquad (1)$$

Second parameter is a relative size of coherent scattering region (CSR), calculated on the basis of Debai–Sherrer equation (Table 2):

$$\Lambda \approx \frac{\lambda}{FWHM \cdot \cos\theta} \qquad (2)$$

This parameter in contrast to the first one depends on FWHM of the XRD spectra lines and is used to estimate comparative characteristic (not absolute) of coherent scattering region of the nanoparticles. FWHM have been calculated as full width at half maximum on Gauss curve that approximate the XRD spectrum lines.

In both equations (1) and (2) the notation θ and stands for the scattering angle and wave length 1.54 mkm, respectively.

One can see (Fig. 3) that interplanar spacing of crystalline lattice of ZnO nanoparticles in *Sample* N1 (5% Mn) are slightly shifted to the lower values in comparison with the ones for N3, N6 and ASTM. Since the nanoparticles contain low amount of the manganese (<1%) thus it hardly could change the lattice parameters of ZnO because of bigger ion radii of Mn^{+2} (0.8 nm) opposite to the ion radii Zn^{2+} (0.73 nm). However such

Table 2. **Relative value of coherent scattering region of three *Samples* N1, N3 and N6 calculated by equation (2)**

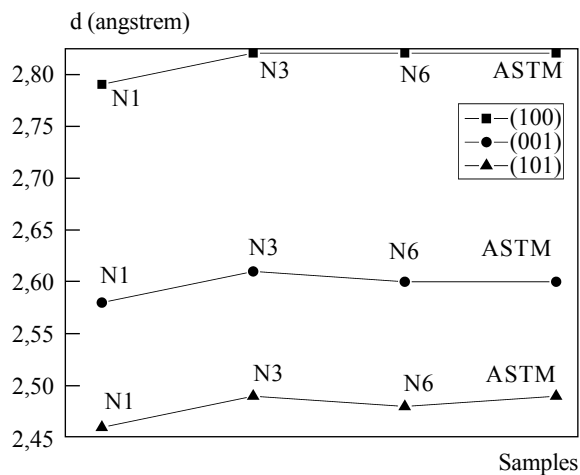| Coherent Scattering Region (Å)	ZnO (100)	ZnO (002)	ZnO (101)
N1	2.07	2.46	2.02
N3	2.25	2.25	2.16
N6	2.49	3.30	2.49

d (angstrem)

Fig. 3. comparative values of interplanar spacing of *Samples* N1, N3, N6 and corresponding ASTM value for three different directions

behavior can be explained if we take into account an effect of surface tension on periods of the crystalline structure. For nanoparticles where surface to volume ratio is high, crystalline structure is strongly affected by surface tension that results in decreasing of the periods of the crystalline lattice. In addition the dimension of the coherent scattering region (Table 2) for these three *Samples* has similar dependence except for the (002) case. Thus basing on these facts we can assume that average size of NPs ZnO:Mn N1 is smaller than NP N3 and N6.

ESR measurements

Due to half-filled *d* shell ($3d^5$) with spin $S = 5/2$, angular momentum $L = 0$ and nucleus spin $I = 5/2$, the resonance of an isolated Mn^{2+} ion located substitutionally on a Zn site in hexagonal ZnO is described by the spin Hamiltonian:

$$H = g\mu_B \vec{H}\vec{S} + A_{ij}S_iI_j + D_{ij}S_iS_j \quad (3)$$

At low concentration (<0.1%) Mn doped ZnO single crystals, an isotropic Zeeman (first term eq. 3) and hyperfine interaction (second term eq. 3) were observed ($g = 2.0016$, $|A| = 76 \cdot 10^{-4}$ cm^{-1}) together with an axial fine structure splitting ($D = 217 \cdot 10^{-4}$ cm^{-1}) [6]. In the case of randomly oriented nanocrystals anisotropic contributions are washed out and one can expect a six line spectrum with a hyperfine splitting (hereafter HFS) of about $76 \cdot 10^{-4}$ cm^{-1} from isolated Mn^{2+} incorporated in the single crystal ZnO.

ESR measurements were used to investigate a behavior of Mn^{2+} in the host material ZnO. ESR spectrums for five *Samples* are given on Fig. 5. It shall be noted that ESR spectra for *Samples* N1 is not resolved thus it is not given in this article. According to these measurements two spectrum patterns can be highlighted:

S1 – broad background line that inhere for all ESR spectrums (dash-dotted lines on the Fig. 5) is related to the exchange and dipole-dipole interaction of Mn between nearby magnetic centers. This line can be attributed to the unknown phase MnO_x (Fig. 2);

S2 – six lined hyperfine structure with mean constant of HFS (CHFS) <A> = (94±3)·10^{-4} cm^{-1} is related to the isolated Mn in ZnO lattice. Value
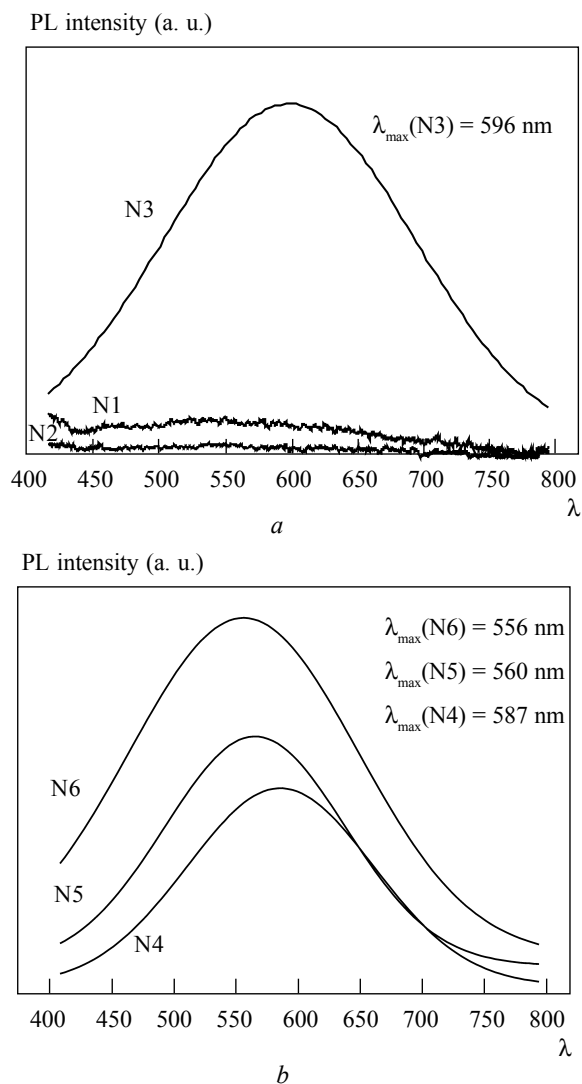
PL intensity (a. u.)

$\lambda_{max}(N3) = 596$ nm

N3

N1

N2

a

PL intensity (a. u.)

$\lambda_{max}(N6) = 556$ nm

$\lambda_{max}(N5) = 560$ nm

$\lambda_{max}(N4) = 587$ nm

N6

N5

N4

b

Fig. 4. PL spectra for *Samples* (*a*) N1–3 and (*b*) N4–6.

Fig. 5. ESR spectrum for (*a*) *Samples* N2–6 at *T* = 300 K

of the constant of HFS is given as «almost equal» because it is mean value over all six lines. Detailed estimation of this value gives confidence interval as ±3. However it is crude approximation but for our objectives and conclusion it is enough.

In hexagonal ZnO lattice manganese ions that substitute of Zn^{2+} in the single crystal undergo the effect of tetrahedral electrostatic field of the surroundings. In such a case the CHFS of Mn^{2+} is $76 \cdot 10^{-4}$ cm^{-1}, in contrast to observed HFS of Mn in ZnO nanoparticles with considerably higher CHFS ($<A> = (94 \pm 3) \cdot 10^{-4}$ cm^{-1}).
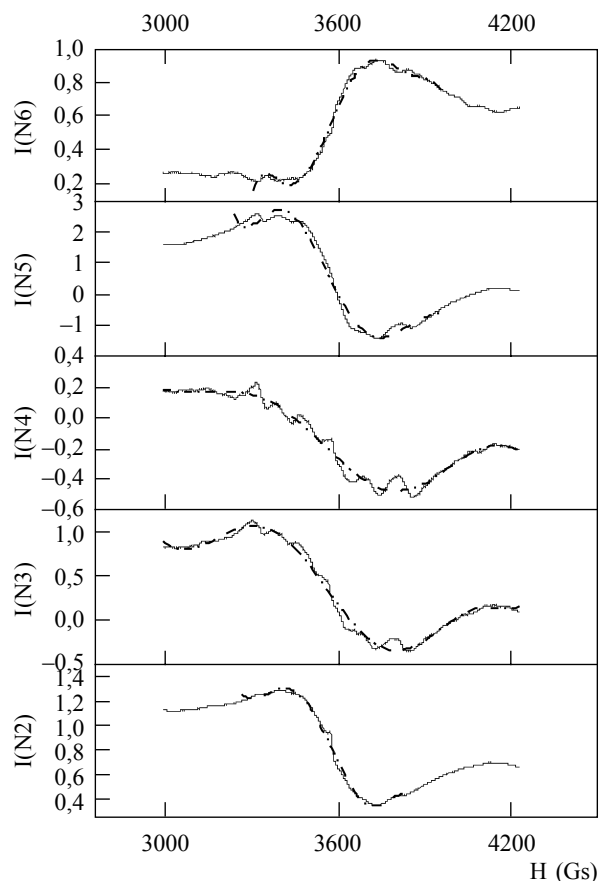
Similar increasing of CHFS for manganese in hexagonal lattice has been observed earlier in nanopowders CdS, ZnS [7–9] and ZnO [10] synthesized in colloidal solution. Such increasing in these works related to formation of cubic $Zn(OH)_2$ crystalline phase on the surface of the nanoparticles. In this structure Mn^{2+} can substitute zinc ions in octahedral surrounding of hydroxide groups. But in our work the synthesis was held under such conditions that exclude formation of any compounds except ZnO and manganese oxides. Thus explanation of such value of CHFS can be related to the disturbances of tetrahedral Zn sublattice at the surface layer of ZnO and formation of octahedral surrounding around manganese ions.

This conclusion is based on the fact that CHFS of Mn in tetrahedral surrounding has lower value than in the case of octahedral one (Table 3). As it can be seen

Table 3. **Comparative table of constants of hyperfine structure for Mn in local octahedral and tetrahedral surrounding**

Octahedral surrounding		Tetrahedral surrounding	
	$A \cdot 10^{-3}$, cm^{-1}		$A \cdot 10^{-3}$, cm^{-1}
ZnF_2	9.6	ZnO	7.4
NaCl	8.2	CdS	6.48
KCl	8.86	CdTe	5.51
NaF	9.1	Al_2O_3	7.5
AgCl	8.1	ZnS	6.4
$SrCl_2$	9.7	–	–

from the table CHFS <A> = $(94\pm3)\cdot10^{-4}$ cm^{-1} lay in the range of the values for octahedral local environment.

These two spectra S1 and S2 are more or less detected for investigated *Samples* N2–6. In particular S1 ESR signal is well observed for whole number of *Samples* that indicate second phase formation (compound with Mn component) for all of them. Sextet structure S2 is weakly resolved for members of second group (N4–6) but nearly absent for *Samples* N1 and N2. The difference between these two groups lays in type of Zn and Mn precursors that are used in chemical synthesis reaction. From this point of view manganese, that is easily oxidized metal, differently acts in nitride and acetate solutions [3]. In second group of precursors the Mn oxidation is more inhibited than in nitrides solution. That leads to increasing of second phase formation in the last medium in comparison with the first one. Therefore one can observe more intensive six lined structure for N4 and N5 than for N1 and N2.

Photoluminescent spectrum

The PL spectrum of bulk ZnO is characterized by two lines. First one lays in UV region 350–370 nm and attributed to the near band gap exciton recombination PL. Second one, wide band line, lies in green-red region of the visible spectrum (500–600 nm) and caused by intrinsic point defects within zinc oxide that lead to appearing of deep and shallow defects levels in the band gap [12–13].

At the transition to nanosized objects the PL spectrum become more ambiguous than in the bulk case. Since influence of surface layer states in such entities is

significantly enhanced with decreasing of their size. Thus it is expected to observe additional lines in the spectrum of nano ZnO attributed to the surface layer. The lines can be varied depending on the shape of the nanoparticles.

On the Fig. 4 spectra of nanoparticles ZnO doped with Mn are shown. All *Samples* are characterized by UV component (~370 nm) that is poor resolved on the UV band of nitrogen laser background (this line is not shown on the pictures). In addition wide band in visible region of the spectrum (500–600 nm) is observed too. The significant widening of this line is clearly attributed to wide distribution of the emission spectrum of the individual nanoparticle within any of the *Samples*. Characteristic dimensions of these nanoparticles is decreased enough that their shape and dimensions have significant influence on the optical transitions.

For the *Samples* N1–2 the intensity of the lines in visible region lies at the noise level. In these nanoparticles the radiationless transition is dominated. But as for the *Samples* with higher manganese content there is intensive line of emission centered at the 590 nm (Fig. 4a). Similar picture is observed for Samples N4–6, the *Samples* with the highest manganese content show the most intensive line in the visible region (Fig. 4b).

There is not enough information to definitely conclude about origin of these lines, but some assumption can be made. Whereas the band line strongly overlap region of defect emission that attributed to the native point defects in ZnO [12], we can make assumption that one of the sources of the green emission is these point defects. That is even in the *Samples* N1–2 there are low resolved picks in 530 nm. Other sources of the emission are assumed to be surface states that depend on manganese content at the surface layer of the nanoparticles. Absence of the isolate manganese in the *Samples* N1–2 is also confirmed by ESR measurements. For other *Samples* where isolate manganese was found by ESR, the PL spectrum have been observed. Therefore we can assume that manganese ions participate in forming or modification of the ZnO defects on the surface level and in some way promote emission in visible region of the spectrum.

The role of the manganese as surface agent, but not luminescence center itself is proved by different position of the PL lines for the *Samples* with different manganese contents. However luminescence of the manganese (580 nm) could not be eliminated.

Conclusions

Within this work nanoparticles ZnO doped with Mn immobilized in polyethylene matrix with average size 3–5 nm were synthesized. Two different localizations of Mn have been revealed. First one is localization at the surface layer substituting zinc in cation sublattice ($<A> = (94\pm3)\cdot10^{-4}$ cm^{-1}) that differ from constant of hyperfine structure for ZnO $76\cdot10^{-4}$ cm^{-1}. The second one is thought to form undefined phase MnO$_x$ with unresolved hyperfine structure. Under nitrogen laser excitation (337 nm) visible emission in the range 500–600 nm has been observed that is attributed to defect surface states that are predominant in the nanoparticles.

Отримано наночастинки ZnO:Mn розміром 3–5 нм. За допомогою методів ЕПР, рентгеноструктурного аналізу та фотолюмінесценції досліджували структуру цих наночастинок із вмістом марганцю 5, 10 і 20% щодо вихідного розчину прекурсорів. Показано, що переважна кількість марганцю формує другу фазу та заміщує цинк у катіонній підрешітці в поверхневому прошарку цих наночастинок. Середнє значення константи надтонкої структури ($<A> = (94\pm3)\cdot10^{-4}$ cm^{-1}), отримане методом ЕПР, виявилося більшим за очікуване та відмінним від довідникового для марганцю в кристалічній решітці ZnO ($76\cdot10^{-4}$ cm^{-1}). Фотолюмінесцентні вимірювання виявили широку лінію випромінювання в зелено-червоній області спектра 500–600 нм із різним положенням максимуму залежно від типу зразка.

Ключові слова: *наночастинка, ZnO, Mn, фотолюмінесценція, люмінесценція, ЕПР*

Получены наночастицы ZnO:Mn размером 3–5 нм. С помощью методов ЭПР, рентгеноструктурного анализа и фотолюминесценции исследовалась структура этих наночастиц с содержанием марганца 5, 10 и 20% относительно исходного раствора прекурсоров. Показано, что преимущественное количество марганца формирует вторую фазу и замещает цинк в катионной подрешетке в поверхностном слое этих наночастиц. Среднее значение константы сверхтонкой структуры ($<A> = (94\pm3)\cdot10^{-4}$ cm^{-1}), полученное методом ЭПР, оказалось большим по сравнению с ожидаемым и отличным от справочного для марганца в кристаллической решетке ZnO ($76\cdot10^{-4}$ cm^{-1}). Фотолюминесцентные измерения выявили широкую линию излучения в зелено-красной области спектра 500–600 нм с разным положением максимума в зависимости от типа образца.

Ключевые слова: *наночастица, ZnO, Mn, фотолюминесценция, люминесценция, ЭПР*

1. *Klingshirn C.F.* ZnO: From basics towards applications // Phys. Stat. Sol. B. – 2007. – **244**, N 9. – P. 3027–3073.

2. *Bryan J.D., Gamelin D.R.* Doped semiconductor nanocrystals: synthesis, characterization, physical properties and applications // Progress in Inorganic Chemistry – John Wiley & Sons, Inc. – 2005, Vol. 54, pp. 47–126.

3. *Synthesis* of colloidal Mn^{2+}:ZnO quantum dots and High-T$_c$ ferromagnetic nanocrystalline thin films / Norberg N.S., Kittilstved K.R., Amonette J.E. et al. // J. Am. Chem. Soc. – 2004. – **126**, N 30. – P. 9387–9398.

4. *Synthesis* and structure of composition materials on base of nanoparticles ZnO in polyethylen matrix / Kosobudsky I.D., Ushakov N.M., Yurkov G.Yu. et al. // Russian Journal of Inorganic Chemistry. – 2005. – **41**, N 11. – P. 1330–1335.

5. *Nanomaterials* for high density magnetic data storage / Gubin S.P., Spichkin Yu.I., Yurkov G.Yu. et al. // Russian Journal of Inorganic Chemistry. – 2002. – **47**, N 1. – P. 32–67.

6. *Altshuler S.A., Kozjurev B.M.* Electron paramagnetic resonanse of the compounds of the elements of transitions groups. – Nauka, Moscov, 1972, pp. 20–395.

7. *Symmetry* and electronic structure of the Mn impurity in ZnS nanocrystals / T.K. Kennedy, E.R. Glaser, P.B. Klein, R.N. Bhargava // Phys. Rev. B. – 1995. – **52**, N 20. – P. R14356–R14359.

8. *Effect* of Mn^{2+} concentration in ZnS nanoparticles on photoluminescence and electron-spin-resonance spectra / Borse P.H., Srinivas D., Shinde R.F. et al. // Phys. Rev. B. – 1999. – **60**, N 12. – P. 8659–8664.

9. *CdS:Mn nanocrystals* in transparent xerogel matrices: synthesis and luminescene properties / G. Counio, S. Esnouf, T. Gacoin, J.-P. Boilot // J. Phys. Chem. – 1996. – **100**, N 51. – P. 20021–20026.

10. *Magnetic* resonance investigation of Mn^{2+} in ZnO nanocrystals / Huijuan Zhou, D.M. Hofmann, A. Hofstaetter, B.K. Meyer // J. Appl. Phys. – 2003. – **94**, N 3. – P.1965–1969.

11. *Paramagnetic* centers in nanosized oxide powders // Shevchuk V.N., Popovich D.I., Usatenko Yu.M. et al. // Physics and Chemistry of Solid State. – 2009. – **10**, N 2. – P. 289–294.

12. *A comprehensive* review of ZnO materials and devices / Ozgur U., Alivov Ya.I., Liu C. et al. // J. Appl. Phys. – 2005. – **98**, N 4. – P. 041301–041404.

13. *Zinc Oxide* – A Material for Micro- and Optoelectronic Applications / Karpina V.A., Khranovskyy V.D., Lazorenko V.I. et al. – Springer, 2005 – Series II: Mathematics, Physics and Chemistry. – Vol. 194, pp. 59–68.